Chemical Science

EDGE ARTICLE

View Article Online
View Journal | View Issue

Cite this: *Chem. Sci.*, 2017, **8**, 2790

Molecular catalysis at polarized interfaces created by ferroelectric $BaTiO_3$†

Eugene S. Beh,‡[a] Sergey A. Basun,[bc] Xiaofeng Feng,§[a] Ighodalo U. Idehenre,[bd] Dean R. Evans[b] and Matthew W. Kanan*[a]

Received 14th November 2016
Accepted 17th January 2017

DOI: 10.1039/c6sc05032h

www.rsc.org/chemicalscience

The local environment at polarized solid–liquid interfaces provides a unique medium for chemical reactions that could be exploited to control the selectivity of non-faradaic reactions. Polarized interfaces are commonly prepared by applying a voltage to an electrode in an electrolyte solution, but it is challenging to achieve high surface charge densities while suppressing faradaic reactions. Ferroelectric materials have permanent surface charge densities that arise from the dipole moments of ferroelectric domains and can be used to create polarized solid–liquid interfaces without applying a voltage. We studied the effects of ferroelectric oxides on the selectivity of a Rh porphyrin-catalyzed carbene rearrangement. The addition of ferroelectric $BaTiO_3$ nanoparticles to the reaction solution changed the product ratio in the same direction and by a similar magnitude as performing the reaction at an electrode–electrolyte interface polarized by a voltage. The results demonstrate that colloidal suspensions of $BaTiO_3$ nanoparticles act as a dispersible polarized interface that can influence the selectivity of non-faradaic reactions.

Introduction

The double layer region at a polarized solid–liquid interface has electrostatic and chemical properties that differ significantly from a bulk solution.[1,2] These properties affect the rates of electrochemical and photocatalytic reactions, which entail charge transfer across the interface.[3–6] We previously investigated the effects of a polarized electrode–electrolyte interface on the selectivity of catalytic non-faradaic reactions.[7,8] These experiments employed a custom reaction vessel—the "parallel plate cell"—whose walls consist of Si electrodes coated with thin layers of an insulating oxide. Polarization of the oxide–electrolyte interface by applying a voltage across the Si electrodes was found to change the selectivity of reactions confined to the interface, including an epoxide rearrangement catalyzed by Al_2O_3 and an intramolecular carbene rearrangement catalysed by Rh porphyrins. The selectivity changes were dependent on the charge density at the oxide–electrolyte interface, which was determined from the applied voltage and the interfacial capacitance.

The study of non-faradaic reactions at voltage-polarized interfaces has limitations. The need to block faradaic processes necessitates fabricating electrodes with thin insulating layers and dielectric breakdown of these layers limits the maximum interfacial charge density that can be achieved. To address these issues, we sought to replace an electrode polarized by a voltage with a material that permanently has a large surface charge density. Inorganic ferroelectrics are crystalline materials composed of domains that have permanent dipole moments below a characteristic Curie temperature.[9] The surfaces of ferroelectric particles have regions of high charge density where the dipole moment of the domain at the surface has a normal component, leading to the formation of double layers.[10] Previous studies of chemical reactivity at ferroelectric surfaces have utilized the polarization to localize and enhance photoredox reactions.[11–14] We hypothesized that ferroelectric materials would provide polarized solid–liquid interfaces that affect the selectivity of non-faradaic reactions in the same manner as an electrode–electrolyte interface polarized by a voltage (Fig. 1).

Barium titanate ($BaTiO_3$) is a readily accessible ferroelectric metal oxide with a Curie temperature of 120 °C.[15] The polarization of domains in $BaTiO_3$ arises from a small displacement of the Ti^{4+} cation from the centre of the tetragonal unit cell. The polarization of $BaTiO_3$ is stable at room temperature.[16–18]

[a]*Department of Chemistry, Stanford University, 337 Campus Drive, Stanford, California 94305, USA. E-mail: mkanan@stanford.edu*

[b]*Air Force Research Laboratory, Materials and Manufacturing Directorate, Wright-Patterson Air Force Base, Ohio 45433, USA*

[c]*Azimuth Corporation, 4134 Linden Avenue, Suite 300, Dayton, Ohio 45432, USA*

[d]*University of Dayton, Department of ECE and Electro-Optics Program, Dayton, Ohio 45469, USA*

† Electronic supplementary information (ESI) available. See DOI: 10.1039/c6sc05032h

‡ Current address: Department of Chemistry and Chemical Biology, Harvard University, 12 Oxford Street, Naito 118, Cambridge, Massachusetts 02138, USA.

§ Current address: Department of Physics, University of Central Florida, Orlando, Florida 32816, USA.

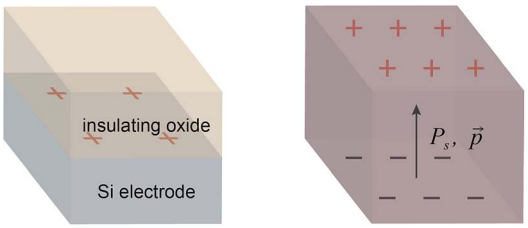

Fig. 1 Depiction of the surface of a charged electrode coated with an insulating oxide (left) and a permanently polarized ferroelectric domain (right). The arrow denotes the direction of polarization of the domain.

The charge density on a $BaTiO_3$ surface that is normal to the dipole moment of a polarized domain can be estimated from previous measurements of the spontaneous polarization (P_s) of $BaTiO_3$ nanoparticles. The P_s of a $BaTiO_3$ nanoparticle composed of a single ferroelectric domain corresponds to the charge densities on the opposing surfaces of the domain that are normal to the dipole moment (Fig. 1). Ball milling of bulk $BaTiO_3$ powder produces nanoparticles that are composed of a small number of ferroelectric domains. We have measured P_s values of 20–120 μC cm^{-2} for ball milled $BaTiO_3$ nanoparticles by performing triangular wave ac voltammetry on nanoparticle suspensions.[19,20] (These values for P_s assume that each nanoparticle is a cube composed of a single ferroelectric domain; particle aggregation will lower the observed P_s).[21,22] Notably, surface charge densities of 20–120 μC cm^{-2} are considerably larger than what is accessible in the parallel plate cell at voltages below the dielectric breakdown limit (at most ~14 μC cm^{-2}).[8] Larger $BaTiO_3$ particles that have not been subjected to ball milling have little or no measurable P_s because they are composed of many ferroelectric domains that are randomly oriented and therefore cancel each other out. Nevertheless, the average magnitude of surface charge density on large $BaTiO_3$ particles is expected to be similar to $BaTiO_3$ nanoparticles because the charge density at any point on the surface is dominated by the orientation of the closest domain.

Results and discussion

A Rh porphyrin-catalyzed intramolecular carbene reaction was used as a model reaction. Diazoketone **1** reacts at ambient temperature with Rh porphyrin catalysts to form a mixture of products **2** and **3** (Scheme 1). In the absence of a polarized interface, the reaction favours **2** over **3** by an approximately 10 : 1 ratio. We previously studied this same reaction in the parallel plate cell using an applied voltage to create polarized electrode–electrolyte interfaces.[8] Rh porphyrin catalysts were localized to these interfaces using either covalent attachment or spontaneous physisorption. With Al_2O_3-coated electrodes or alkylphosphonate-coated electrodes, the **2** : **3** ratio decreased as the magnitude of the voltage was increased, reaching 2 : 1 at the maximum voltage that could be applied before dielectric breakdown. We attributed this change to an effect of the local solvation and electrostatic environment at the polarized interface on the competing activation barriers leading to **2** and **3**.

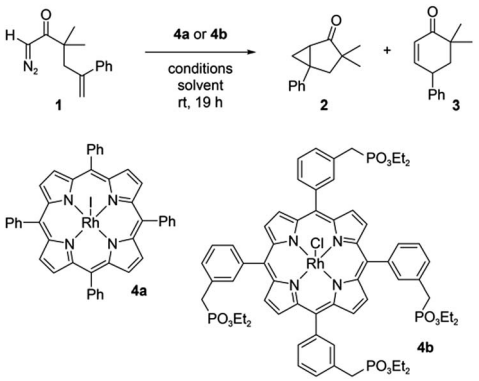

Scheme 1 The reaction of diazo compound **1** catalyzed by Rh porphyrins **4a** or **4b** produces products **2** and **3**.

To see whether the effect of an interface polarized by a voltage could be recapitulated by a dispersed, permanently polarized interface, we compared the selectivity of the Rh porphyrin-catalyzed reaction of **1** to products **2** and **3** in the presence or absence of various ferroelectric ($BaTiO_3$, $PbTiO_3$, and $LiNbO_3$) and non-ferroelectric ($CaTiO_3$, $SrTiO_3$, and TiO_2) nanoparticles. The nanoparticle samples were produced as colloidal suspensions by ball milling the corresponding bulk powders in the presence of heptane and oleic acid.[19] Transmission electron microscopy (TEM) analysis indicated average particle sizes in the range of 7–10 nm for all the milled materials except for $LiNbO_3$ (50 nm; Fig. S1–S12†). The average P_s for the nanoparticles was calculated from the ac displacement current of nanoparticle suspensions subjected to a periodic ac electric field within a narrow cell.[20] A P_s of 20 μC cm^{-2} was measured for the $BaTiO_3$ nanoparticles, indicating substantial alignment of the ferroelectric domains. As expected for non-ferroelectric materials, the P_s values calculated from the ac displacement measurements for $CaTiO_3$, $SrTiO_3$, and TiO_2 were all at least two orders of magnitude smaller than $BaTiO_3$ (Fig. S13†).

Reactions were performed by diluting freshly ball milled 20 : 1 : 1 w/w/w heptane/oleic acid/nanoparticle suspensions to the appropriate nanoparticle concentration with a solution of Rh porphyrin catalyst **4a** in CH_2Cl_2, followed by a solution of **1** in CH_2Cl_2. The reactions were allowed to proceed for 19 h and then analysed using NMR and HPLC. **2** and **3** were the only major products observed (see ESI main text and Fig. S14†).

Fig. 2 shows the **2** : **3** product ratio for reactions performed with different concentrations of $BaTiO_3$ nanoparticles, **1**, and **4a** in CH_2Cl_2. In the absence of nanoparticles, the **2** : **3** ratio was ~11 : 1 in all cases. The largest changes were observed with 0.2 mM **1** and 0.2 μM **4a**, to which the addition of increasing concentrations of $BaTiO_3$ nanoparticles up to 1 mg mL^{-1} resulted in a 5.1-fold decrease of the product ratio from 10.7 : 1.0 to a minimum of 2.1 : 1.0. These changes are in the same direction as what was observed with externally polarized electrode–electrolyte interfaces in the parallel plate cell.[8] Smaller changes were observed with higher ratios of catalyst to nanoparticles, most likely because of incomplete localization of the catalyst to the ferroelectric–solution interface (see below).

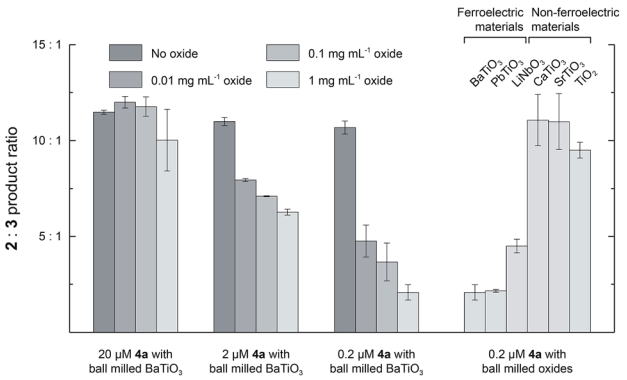

Fig. 2 The dependence of product ratio **2** : **3** on the catalyst **4a** concentration and ball milled oxide concentration. All reactions were conducted with 2 mM of **1** in CH_2Cl_2 at room temperature for 19 h (0.2 mM of **1** when catalyst concentration is 0.2 μM). Data are averaged over two or three separate experiments; error bars represent the standard deviation in the observed product ratio.

Under the same conditions with 1 mg mL^{-1} of nanoparticles, similar changes in the product ratio were also seen with other ferroelectric materials like $PbTiO_3$ (2.1 : 1.0) and $LiNbO_3$ (4.5 : 1.0). In contrast, very little effect on the product ratio was seen with chemically similar non-ferroelectric nanoparticles such as $CaTiO_3$ (11.1 : 1.0), $SrTiO_3$ (11.0 : 1.0), or TiO_2 (9.5 : 1.0).

Control experiments in which **1** was combined with $BaTiO_3$ nanoparticles in the absence of catalyst **4a** showed no conversion, which shows that the $BaTiO_3$ is not itself a catalyst for the diazo decomposition. In addition, reactions performed in the presence of heptane and oleic acid without any nanoparticles gave a **2** : **3** ratio of 11.3 : 1.0, indicating that these additives themselves do not impact the product ratio.

The ability of the polarized $BaTiO_3$–solution interface to affect the selectivity of **4a** requires that a substantial portion of the catalyst partitions at or near the $BaTiO_3$ surface during the reaction. The concentration dependence of the $BaTiO_3$ effect in the results above is consistent with an interface-dependent effect: as the ratio of $BaTiO_3$ surface area to **4a** is increased, a larger change in product ratio is observed. Notably, the surface coverage of long aliphatic capping ligands at colloidal nanoparticles is much lower than one monolayer,[23] which may be critical to allow the reactant and catalyst molecules to localize near the surface.

To further test this model, a reaction was performed in the presence of an excess of un-metalated 5,10,15,20-tetraphenylporphyrin (TPP), which could compete with **4a** for localizing to the surface. When 100 μM TPP was added to a reaction with 2 mM **1**, 2 μM **4a** and 1 mg mL^{-1} of $BaTiO_3$ nanoparticles, the product ratio was 10.6 : 1.0 compared to 6.3 : 1.0 when TPP was omitted and 11.0 : 1.0 when both TPP and $BaTiO_3$ were absent. This result shows that the $BaTiO_3$ effect is lost in the presence of a species that can block the surface localization of the catalyst. Furthermore, when 2 μM **4a** was first stirred with 1 mg mL^{-1} of $BaTiO_3$ nanoparticles for 24 h before the introduction of 100 μM TPP and 2 mM **1**, the ratio was 10.2 : 1.0 after a further 19 h of reaction time. This experiment demonstrates that simply exposing the catalyst to $BaTiO_3$ nanoparticles does not result in an irreversible change to a species with different selectivity. Notably, if the anion of **4a** is replaced by chloride, a smaller change in product ratio from 8.1 : 1.0 (no $BaTiO_3$) to 5.1 : 1.0 (1 mg mL^{-1} $BaTiO_3$) is obtained, which may reflect reduced localization of the Cl-bound Rh porphyrin at the $BaTiO_3$ surface.

In order to understand the timescale on which ferroelectric nanoparticles affect the catalyst, the reaction kinetics were studied in the presence or absence of the various ball milled ferroelectric oxides (Fig. 3). Solutions of 2 mM **1**, 2 μM **4a**, and 1 mg mL^{-1} of ball milled oxide ($BaTiO_3$, $PbTiO_3$, or $LiNbO_3$) in approximately 10 mL of CH_2Cl_2 were prepared, as well as an identical reaction with no oxide. Ball milled oxides were used within 60 minutes after ball milling had concluded. Over the course of 96 h, aliquots from each of the reaction mixtures were quenched with acetonitrile and immediately analysed by HPLC to determine the conversion and ratio of products **2** and **3**. In each case, the product ratio stayed roughly constant throughout the course of 96 h, which suggests that catalyst molecules localize to the polarized ferroelectric surface within, at most, several hours. The slight increase in product ratio after the 6 h mark is attributed to some aggregation of the ball milled nanoparticles over the course of several hours, which resulted in a lowered surface area that was accessible to the catalyst.

The effect of $BaTiO_3$ nanoparticles was also examined in solvents other than CH_2Cl_2. Reactions were performed with 2 mM **1** and 2 μM **4a** in $PhCF_3$, THF, EtOAc, and $PhCH_3$. In the absence of $BaTiO_3$ nanoparticles, the **2** : **3** ratio ranged from 9.4 : 1.0 to 17.9 : 1.0, demonstrating that the strong preference for cyclopropanation is maintained across diverse solvents. The addition of 1 mg mL^{-1} $BaTiO_3$ nanoparticles caused a reduction in the **2** : **3** ratio in all cases, with a substantial variation in the magnitude of the effect (Fig. 4). The largest effect was a 6.6-fold reduction from 17.9 : 1.0 to 2.7 : 1.0 observed in THF. Solvents more polar than $PhCF_3$ could not be used because they caused immediate flocculation of the nanoparticles.

Unmilled $BaTiO_3$ particles have no measurable P_s because they are composed of randomly oriented domains (see above),

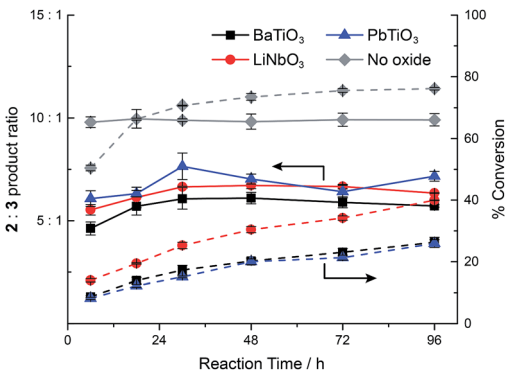

Fig. 3 Evolution of the conversion (right axis, dashed lines) and product ratio **2** : **3** (left axis, solid lines) with time in the presence or absence of various ball milled ferroelectric oxides. Aliquots were taken from reactions that were run with 2 mM **1** and 2 μM **4a** in CH_2Cl_2 at room temperature. Ball milled oxide, if present, is used at a concentration of 1 mg mL^{-1}.

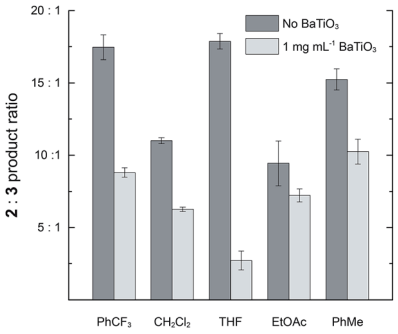

Fig. 4 The effect of adding 1 mg mL^{-1} ball milled $BaTiO_3$ nanoparticles on the product ratio **2** : **3** in a variety of solvents. Reactions were run with 2 mM **1** and 2 μM **4a** at room temperature for 19 h.

but they still have regions of high surface charge densities. Adding 1 mg mL^{-1} of unmilled $BaTiO_3$ particles to a reaction with 2 mM **1** and 2 μM **4a** caused only a 1.2-fold reduction in the **2** : **3** ratio, but the surface area of these relatively large particles (~900 nm) is too low for effective physisorption of **4a** in solution. To test for an interfacial polarization effect on selectivity with unmilled $BaTiO_3$, we prepared Rh porphyrin **4b** with four phosphonate groups to enable covalent surface attachment. The results of reactions performed with **4b** are summarized in Fig. 5. When used as a homogeneous catalyst, 2 μM **4b** reacted with 2 mM **1** in CH_2Cl_2 to give a **2** : **3** product ratio of 8.8 : 1.0. As with catalyst **4a**, the introduction of 1 mg mL^{-1} ball milled $BaTiO_3$ resulted in a 2.0-fold decrease of the product ratio to 4.5 : 1.0. Next, **4b** was attached to various ferroelectric and non-ferroelectric oxides studied. Reactions performed with 2 mM **1** and 1 mg mL^{-1} unmilled $BaTiO_3$ functionalized with **4b** gave a **2** : **3** product ratio of 2.2 : 1.0, corresponding to a 4.0-fold reduction. The **2** : **3** ratio was further reduced to 1.8 : 1.0 if the $BaTiO_3$ functionalized with **4b** was first subjected to ball milling and then used at the same oxide concentration.

In contrast, when **4b** was attached to the non-ferroelectric oxides TiO_2, $CaTiO_3$, and $SrTiO_3$, a small (1.4-fold) effect on the reaction to approximately 6.3 : 1 was observed. Measurements of zeta potentials for TiO_2 particles in hexane in the presence of surfactant indicate surface charge densities on the order of −0.1 μC cm^{-2}, which is much lower than the surface charge density for ferroelectric nanoparticles.[24] The small change in selectivity observed upon attachment of **4b** to nonferroelectric nanoparticles may arise from the interaction of the catalyst with the oxide surface or a subtle conformational biasing for attached catalysts.[25,26] When **4b** was attached to ferroelectric $PbTiO_3$, the ratio was 5.3 : 1.0, which was only slightly lower than the other non-ferroelectric oxides. This result may arise from decreased robustness of the phosphonate linkage to the $PbTiO_3$ surface and increased leaching of catalyst molecules into the bulk solution. Nevertheless, attachment to ferroelectric oxides, especially $BaTiO_3$, effected a substantially larger change in selectivity than attachment to other non-ferroelectric oxides.

The results above demonstrate that the polarized interface between a ferroelectric oxide and an organic solvent can change the selectivity of catalytic reactions in the same way as an electrically polarized electrode–electrolyte interface. By attaching the catalyst to $BaTiO_3$ surfaces or adding $BaTiO_3$ nanoparticles to the reaction solution, the **2** : **3** ratio is reduced by up to a factor of 4.9. Similar effects are seen with ball milled ferroelectric $PbTiO_3$ and $LiNbO_3$; chemically similar but non-ferroelectric $CaTiO_3$, $SrTiO_3$, or TiO_2 nanoparticles had essentially no effect, which indicates that the selectivity change requires the permanently polarized domains in $BaTiO_3$.

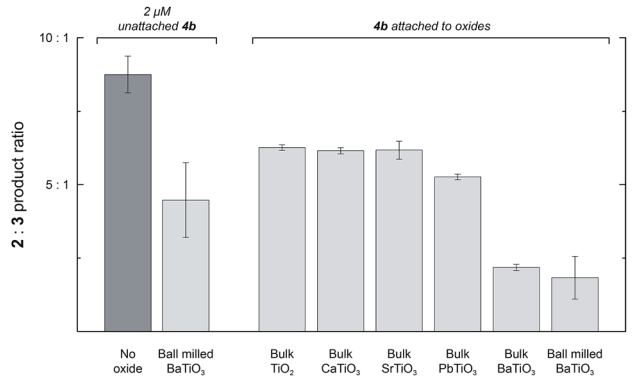

Fig. 5 The product ratio **2** : **3** with catalyst **4b** unattached (2 μM, left two columns) or attached to various titanium-containing oxides (right columns). All reactions were conducted with 2 mM of **1** and 1 mg mL^{-1} of oxides (where present) in CH_2Cl_2 at room temperature. Reaction times were 19 h for all experiments, but 96 h for $CaTiO_3$, $SrTiO_3$, and $PbTiO_3$ in order to obtain sufficient conversion for analysis.

Conclusions

By using ball milled ferroelectric nanoparticles such as $BaTiO_3$, a polarized interface can now be introduced to a reaction medium without the need for physical electrodes. The use of ferroelectric nanoparticles provides an accessible way to investigate and exploit the effects of interfacial polarization on catalysis.

Acknowledgements

We thank the Air Force Office of Scientific Research (FA9550-14-1-0132) for support of this research.

Notes and references

1 J. O. M. Bockris, A. K. N. Reddy and M. Gamboa-Aldeco, in *Modern Electrochemistry Volume 2*, Springer, US, 1970, pp. 623–843.
2 R. Parsons, *Chem. Rev.*, 1990, **90**, 813–826.
3 A. J. Bard and L. R. Faulkner, *Electrochemical Methods: Fundamentals and Applications*, John Wiley & Sons, New York, 2001.
4 E. Gileadi, *Electrode Kinetics for Chemists, Engineers, and Materials Scientists*, Wiley-VCH, New York, 1993.
5 E. J. F. Dickinson and R. G. Compton, *J. Electroanal. Chem.*, 2011, **661**, 198–212.
6 S. Chen, Y. Liu and J. Chen, *Chem. Soc. Rev.*, 2014, **43**, 5372–5386.

7 C. F. Gorin, E. S. Beh and M. W. Kanan, *J. Am. Chem. Soc.*, 2012, **134**, 186–189.
8 C. F. Gorin, E. S. Beh, Q. M. Bui, G. R. Dick and M. W. Kanan, *J. Am. Chem. Soc.*, 2013, **135**, 11257–11265.
9 M. J. Polking, M. G. Han, A. Yourdkhani, V. Petkov, C. F. Kisielowski, V. V. Volkov, Y. Zhu, G. Caruntu, A. P. Alivisatos and R. Ramesh, *Nat. Mater.*, 2012, **11**, 700–709.
10 R. J. Ferris, S. Lin, M. Therezien, B. B. Yellen and S. Zauscher, *ACS Appl. Mater. Interfaces*, 2013, **5**, 2610–2617.
11 S. V. Kalinin, D. A. Bonnell, T. Alvarez, X. Lei, Z. Hu, J. H. Ferris, Q. Zhang and S. Dunn, *Nano Lett.*, 2002, **2**, 589–593.
12 J. L. Giocondi and G. S. Rohrer, *J. Phys. Chem. B*, 2001, **105**, 8275–8277.
13 M. Stock and S. Dunn, *J. Phys. Chem. C*, 2012, **116**, 20854–20859.
14 Y. Cui, J. Briscoe and S. Dunn, *Chem. Mater.*, 2013, **25**, 4215–4223.
15 S. Roberts, *Phys. Rev.*, 1947, **71**, 890–905.
16 G. H. Kwei, A. C. Lawson, S. J. L. Billinge and S.-W. Cheong, *J. Phys. Chem.*, 1993, **97**, 2368–2377.
17 M. B. Smith, K. Page, T. Siegrist, P. L. Redmond, E. C. Walter, R. Seshadri, L. E. Brus and M. L. Steigerwald, *J. Am. Chem. Soc.*, 2008, **130**, 6955–6963.
18 K. Page, T. Proffen, M. Niederberger and R. Seshadri, *Chem. Mater.*, 2010, **22**, 4386–4391.
19 H. Atkuri, G. Cook, D. R. Evans, C. I. Cheon, A. Glushchenko, V. Reshetnyak, Y. Reznikov, J. West and K. Zhang, *J. Opt. A: Pure Appl. Opt.*, 2009, **11**, 024006.
20 S. A. Basun, G. Cook, V. Y. Reshetnyak, A. V. Glushchenko and D. R. Evans, *Phys. Rev. B: Condens. Matter Mater. Phys.*, 2011, **84**, 024105.
21 D. R. Evans, S. A. Basun, G. Cook, I. P. Pinkevych and V. Y. Reshetnyak, *Phys. Rev. B: Condens. Matter Mater. Phys.*, 2011, **84**, 174111.
22 P. Lagos, R. Hermans, N. Velasco, G. Tarrach, F. Schlaphof, C. Loppacher and L. M. Eng, *Surf. Sci.*, 2003, **532**, 493–500.
23 C. N. Valdez, A. M. Schimpf, D. R. Gamelin and J. M. Mayer, *ACS Nano*, 2014, **8**, 9463–9470.
24 M. Kosmulski, P. Próchniak and J. B. Rosenholm, *Colloids Surf., A*, 2009, **348**, 298–300.
25 C. M. Queffélec, M. Petit, P. Janvier, D. A. Knight and B. Bujoli, *Chem. Rev.*, 2012, **112**, 3777–3807.
26 J. M. Notestein and A. Katz, *Chem.–Eur. J.*, 2006, **12**, 3954–3965.